

To appear in:

Journal of Theoretical and Applied Physics

Online ISSN: 2251-7235

Print ISSN: 2251-7227

This PDF file is not the final version of the record. This version will undergo further copyediting, typesetting, and production review before being published in its definitive form. We are sharing this version to provide early access to the article. Please be aware that errors that could impact the content may be identified during the production process, and all legal disclaimers applicable to the journal remain valid.

Received: 30 January 2026

Revised: 30 March 2026

Accepted: 26 April 2026



DOI: <https://doi.org/10.57647/jtap.2026.2005.04>

Research Article

Partial Stopping Power Effective Charge of Hydrogen Di-cluster Ions in Al_2O_3 and ZnO Compound

Zainab Shakir Naser, Ishraq Ahmed Shakir*, Zainab H. Baqi

Department of Physics, College of Science, Mustansiriyah University, Baghdad, Iraq

*Corresponding Author: ishraqahmed96@uomustansiriyah.edu.iq

ORCID: <https://orcid.org/0000-0002-4939-6101>

ABSTRACT

As Self-points. This paper is on the theoretical investigation of full C in the Light Radius of hydrogen cluster ions; how fast they pass through two compound targets such as Al_2O_3 or ZnO. The calculations were done using Bragg's additivity rule for compounds, a description of the projectile charge distribution due to Brandt and Kitagawa and an approximate representation of target plasma response using the plasmon pole approximation. So now the stopping effective charge $R(v,e)R(v,e)R(v,e)$ term and the effective partial stopping ejection charge, $\zeta(e)\zeta(e)\zeta(e)$, can be obtained from Eq. (20). Their functional dependence was calculated in analogy to experiments with the internuclear separation $r_0r_0r_0$, charge value q_{qx} and projectile energy E. results show that avoid hole interactions make the total stopping power; small r-region become increasingly prominent with increasing internuclear separations and projectile ionization. Moreover, as the projectile turns close to full ionization state (the correlation effects the importance of the correlation term increases over such parameters) reaches a maximum whereas the partial stopping effective charge evancountry to unity. All differences between Al_2O_3 and ZnO can be put down



to their dissimilar electronic structures and charge density responses. Orbits. This method can be used for predictions on energy transfer and electrolyte state-dependent loss in technology-oriented oxygen compounds by correlated du projectiles, for instance in the ion beam analysis, ion beam projected kuroky bands, and evaluation of radiation damage of functional C semiconducting ceramics. The numerical calculations were performed using FORTRAN-90. With the present results now available as a reference for future experimental benchmarks and the interpretation of cluster-ion media interactions.

Keywords: Stopping Power, Hydrogen di-cluster, Vicinage Effect, Effective Charge, BK- theory, Al_2O_3 , ZnO, Dielectric formalism.

1. Introduction

Cluster ions have attracted much interest. Their energy loss in matter is not just a sum of the losses for ions acting independently at all [1]. When two ions move in some correlations and an internuclear separation exists, this causes interference between induced electronic excitations that has led to the so-called vicinage effect. The projectile's stopping power is thus modified by this effect. It plays an important part in understanding how ions correlated with condensed matter interact. The vicinage effect modifies the projectile's stopping power and plays an important role in understanding how ions correlated with condensed matter interact. Hydrogen clusters are one of the simplest systems for investigating these collective interaction effects theoretically [2].

The stopping power is an essential quantity in estimating the energy deposition, particle range, and charge-state-dependent interactions of solids, though optical properties of the SeO_2 nanoparticles are the focus of several published papers, the preparation methods presented in those papers could offer ideas for future research on ion-beam interactions with nano-sized substances. The results from this work may themselves constitute a starting point [3]. Reliable stopping power data form the backbone of various ion-beam analyses, radiation–matter interaction studies, and accelerator-based materials characterization. After all, once we know where ions are coming from, it becomes much easier to understand the data they produce. We know very little about ions in media that have different environments and structures—even so, this limitation does not prevent effective study practice in most media [4].

Numerous papers show how radiation changes the characteristics of materials. This understanding can be applied to ion-beam interactions, especially when they involve compound targets such as Al_2O_3 and ZnO. In such cases radiation induced property changes will influence stopping power and energy loss behavior [5].

Furthermore, there are many advanced scientific and technological applications. The dielectric formulation is one of the most widely used techniques for characterizing interactions between swift ions and charged particles with the material. In previous work on the inelastic energy loss of fast incident ions in

solids for different projectile-target combinations, many models have been proposed to explain and predict these experimental results [6].

In the present work, Al_2O_3 and ZnO were selected as target materials, as both are technologically important oxides with widespread functional applications. Alumina is extensively employed in catalysis and advanced ceramic systems due to its mechanical strength, structural stability and activity as a catalyst carrier, whereas ZnO is a major semiconductor material that already has established roles in optoelectronic devices and electron-transport layers for solar-cell technologies. Accordingly, both these materials represent good choices for examining how hydrogen di-cluster ions lose energy. One result from the radiation effects is to change material characteristics. This insight can be extended to a study of ion-beam interactions with compound targets, such as Al_2O_3 and ZnO , where radiation effects will affect stopping power material behavior during energy deposition [7].

The present method is intended to be used primarily to theoretically predict the energy deposition spectra that correlated hydrogen projectiles will impart to compound materials as a function of the projectile charge state, velocity, and internuclear separation. These types of predictions are valuable when interpreting experiments with ion beams, refining estimates of energy loss in compound targets, and evaluating irradiation effects in oxide materials applicable to ceramics, semiconductors, and related functional devices. Thus, the current calculations are not only of theoretical interest and represent a robust benchmark for future experimental comparison, but they also produce information that can be used for studies of ion–solid interaction in technologically important materials.

2. Theoretical Basis

First of all, the main process by which heavy charged particles remove their energy in a matter is through their interactions with the electrons of the target medium. The stopping of fast projectiles can be described in the framework of the dielectric formalism, which has been successfully applied for many years to describe inelastic energy loss of ions in solids. In the present work, this framework is applied to provide a proper treatment to the vicinage effects and partial effective charge from the Brandt–Kitagawa approach for the stopping of fast hydrogen di-cluster ions in compound targets [8] statistically.

The stopping power of a projectile, with atomic number z_1 in an electron gas system with a Lindhard function of target description, is given by the following expression:

$$\left(\frac{dE}{dx}\right) = \frac{2z_1^2}{\pi v^2} \int_0^\infty \frac{dk}{k} \int_0^{kv} d\omega \omega \text{Im} \left[\frac{-1}{\epsilon(k, \omega)} \right] \quad (1)$$

For di-cluster ions with atomic numbers Z_1 and Z_2 , the stopping power is modified by the vicinage effect $I(Z_1, Z_2, r_0)$ according to:

$$I(z_1, z_2, r_0) = \frac{2z_1 z_2}{\pi v^2} \int_0^\infty \frac{dk}{k} \frac{\sin kr_0}{kr_0} \int_0^{kv} d\omega \omega \operatorname{Im} \left[\frac{-1}{\epsilon(k, \omega)} \right] \quad (2)$$

Where are two neighboring points charged with an inter-nuclear distance r_0 . Therefore, the stopping power of cluster protons is [9,10]:

$$\left(\frac{dE}{dx} \right)_{clu.} = \left(\frac{dE}{dx} \right)_{self} + I(z_1, z_2, r_0) \quad (3)$$

Where $\left(\frac{dE}{dx} \right)_{self}$ is the stopping power due to self-interaction given in Eq. (1).

Substitute Eqs. (1,2) into Eq. (3) gives,

$$\left(\frac{dE}{dx} \right)_{clu.} = \frac{2}{\pi v^2} \int_0^\infty \frac{dk}{k} \int_0^{kv} d\omega \omega \operatorname{Im} \left[\frac{-1}{\epsilon(k, \omega)} \right] \left[(z_1^2 + z_2^2) + 2z_1 z_2 \frac{\sin kr_0}{kr_0} \right] \quad (4)$$

In a complex target, imitating the same sort of material changes--for example two distinct ways in which stress occurs--can change stopping power and energy deposition behavior [10].

For the stopping power in an electron gas described by the Lindhard dielectric function with a single projectile of atomic number Z_1 , Eq. (1) reflects its effect. In a di-cluster projectile composed of two ions with atomic numbers Z_1 and Z_2 , the stopping power is modified by the spatial correlation between its two constituents. This correlation introduces a vicinage term--as expressed in Eq. (2). which results in a total cluster stopping power as given in Eq. (3). Substituting equations (1) and (2) into Eq. (3) leaves us with the stopping power formula for one atom in the form of Eq. (4). Thus, the total stopping power of the hydrogen di-cluster, where $Z_1=Z_2=1$ consists of two different contributions. The first of these arises from independent interactions of each proton with the medium--whereas interference between the two correlated projectiles itself yields the second one. [11,12]. So,

$$S(v) = n_1 S_1(v) + n_2 S_2(v) \quad (5)$$

Where n_1, n_2 are the number of atoms of each element, and $S_1(v), S_2(v)$ The stopping power of each element.[9]

Bragg's additivity rule was used to evaluate stopping power for compound materials. It assumes that the total stopping power of the compound can be regarded as the sum of contributions from its constituent elements. In this approximation, the stopping powers of Al_2O_3 and ZnO are derived from the stopping powers of the individual atoms being weighted according to their abundance in that compound, as given by Eq. (5). Using this procedure provides a practical way to extend stopping calculations from single elements to compound materials.

2.1. Plasmon Pole Approximation (PPA)

In probing the stopping power, the dielectric response of the particular medium concerned is one of several key inputs. In the fast velocity range, a well-known, reliable, and physically meaningful representation of the dielectric function is given by its single-pole spectrum plasmon approximation. In this model, the response depends on the plasma frequency, the average electronic density, the tau parameters, the effective band-gap contribution to insulators or semiconductors, and the dispersion term associated with density wave propagation in that electron gas. The dissipation factor takes account of the fact that the excitation spectrum has a finite width[12]. The target material's linear-response function is the opener for calculating the stopping power (k, ω). At high velocities where the projectile can excite plasmons in the medium, Echenique and Basbas have used the Plasmon Pole Approximation (PPA) of the dielectric function. (k, ω) :

$$(k, \omega) = 1 + \frac{\omega_p^2}{\omega_g^2 + \beta^2 k^2 + k^4/4 - \omega(\omega - i\gamma)} \quad (6)$$

Where $\omega_p = (3rs/3)^{1/2}$ is the plasmon frequency, rs is the radius of the average volume occupied by each electron in a unit of Bohr, ω_g in semiconductors and insulators, the effective bandgap energy gives a collective resonance frequency, Ω_p which represents

$\Omega_p = (\omega_p^2 + \omega_g^2)^{1/2}$; $\omega_g = 0$ for metal, plasmon dispersion is included through the term containing $\beta = 3kf^2/5$ the propagation of density disturbances in an electron gas and kf is a Fermi level wave number. β^2 refers to the square of kinetic energy, this term used for Single-particle effects are accounted $k^2/2$, of a free electron with momentum (k). γ is a factor that represents damping processes [13,14].

2.2. Partial Stopping Power Effective Charge

To describe this kind of distorting effect, this paper uses the Brandt-Kitagawa statistical model, in it the ionic charge is supposed to result from the difference between nuclear charge and number of bound electrons. The corresponding degree of ionization fraction is labelled by 'q'. When a fast particle passes through material, it also excites electronic excitations and so ionizes those in the target. Meanwhile the stopping power must be corrected so as to include ionic charge density of the projectile. By incorporating a Fourier transform of the projectile (electron) density into the dielectric formulation (1) Here the form of the expression for the stopping power is changed accordingly[15]. Here, the partial stopping effective charge $\zeta(q)$ is defined and calculated for each constitutive element based on the corrected stopping cross-section, and then Bragg's principle is employed to calculate the effective value for compound targets. The statistical model derived by Brandt and Kitagawa (BK)[6, 16,17], in which ionic charge is $Q = Zp - Ne$, and the degree of ionization is:

$$q = \frac{Q}{Z_p} = 1 - (N_e/Z_p) \quad (7)$$

Where N_e refers to the number of electrons engaged to the projectile and Z_p is the atomic projectile number, when a fast projectile moves through substance materials, it induces electronic excitations and ionization in the material, which causes a loss of energy; therefore, Eq. (1) becomes:

$$S(q) = \frac{2}{\pi v^2} \int_0^\infty \frac{dk}{k} |Z_p - \rho_{e,q}(k)|^2 \int_0^{kv} d\omega \omega \text{Im} \left[\frac{-1}{\epsilon(k, \omega)} \right] \quad (8)$$

The electronic density of the projectile

$$|\rho(q) = Z_p - \rho_{e,q}(k)|$$

Where $\rho_{e,q}(k)$ is the Fourier transform of the electron density, $\rho_{e,q}(k) = Z_p \frac{1-q}{1+(k\Lambda)^2}$ [5], therefore,

$$\rho_q(k) = Z_p \frac{q + (k\Lambda)^2}{1 + (k\Lambda)^2} \quad (9)$$

$$\Lambda(Z_p, N_e) = \frac{0.48 N_e^{2/3}}{Z_p - N_e/7} \quad (10)$$

Rewrite Eq. (4) by taking the electron charge density. $\rho_q(k)$ into consideration,

$$\left(\frac{dE}{dx} \right)_{clu.} = \frac{2}{\pi v^2} \int_0^\infty \frac{dk}{k} |\rho_e(k)|^2 \int_0^v d\omega \omega \text{Im} \left[\frac{-1}{\epsilon(k, \omega)} \right] \left[(z_1^2 + z_2^2) + 2z_1 z_2 \frac{\sin kr_0}{kr_0} \right]$$

(11)

Thus, the stopping cross-section of di-cluster ions in charge fraction is $S(q, v)$, and for bare nucleus, $q \rightarrow 1$ is $S(q \rightarrow 1, v)$. The partial stopping effective charge, $\zeta(q)$ It is defined as follows [13,18]:

$$\zeta = \left(\frac{S(q, v)}{S(q, v)} \right)^{1/2} \quad (12)$$

And for each element in the compound, $\xi_i = \left(\frac{S(q, v)}{S(q, v)} \right)^{1/2}$

3. Results and Discussion

The stopping power of a hydrogen di-cluster ion means there are two parts involved, that is, the self-term and the correlation term. In the calculations just made, we handled these quantities as functions of q (fraction ionized), r_0 (internuclear distance), and projectile energy for Al_2O_3 and ZnO compounds. The result leads one to understand directly how some of those present growth laws appear in our quantum medium model. From a comparison of the time scales of localization and de-localization, one can see that characteristic decade-heavy particle motion for different time regimes is governed by transition rates between bands. The results indicate how the charge state and spatial correlation let the cluster behave in hadronic matter media for different kinetic energies of fast H ions at high velocity for two compound targets (Al_2O_3 and ZnO) is shown using Eq. (4). The results were as in Fig. 1:

Fig. 1 compares the self and correlation stopping powers of fast Al_3 hydrogen di-cluster ions for ZnO at a projectile energy of 0.05 MeV. In both compounds, the self-stopping contribution is large compared to any correlational contribution over most of the ionization range (in particular, as the charge fraction approaches 1). The difference between the two terms reflects the different electronic responses of the two target materials. The results also suggest that at low ionization fractions the gap between self and correlation stopping falls off; there is an approach of the two contributions toward one another.

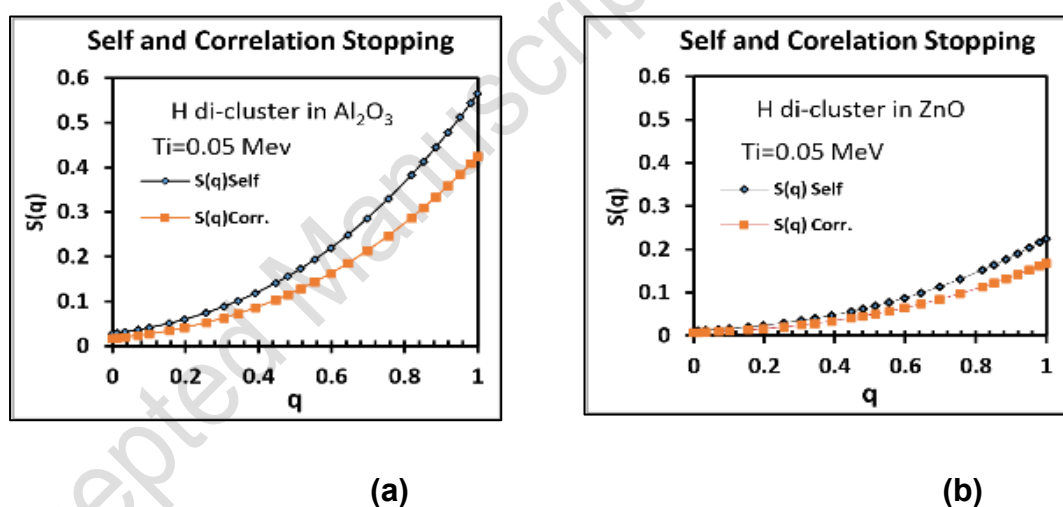


Fig. (1): Self and correlation stopping power for fast Hydrogen di-cluster ions at ($T_i=0.05\text{MeV}$)

In Fig. 2, the correlation stopping power is plotted as a function of internuclear distance r_0 for several charge fractions of Al_2O_3 and ZnO . It is clear from the results that the correlation term decreases as one moves the protons apart. This is consistent with a weaker vicinage effect: as you pull the protons further and

further away from each other, they tend to be less aware of what's happening around them. For ZnO, the correlation contribution is still relatively small for low charge fractions however it starts to rise and becomes noticeable when the nucleus reaches higher ionization states. This behavior provides affirmation that the vicinage effect is most pronounced among cluster components whose closely-spaced and highly ionized.

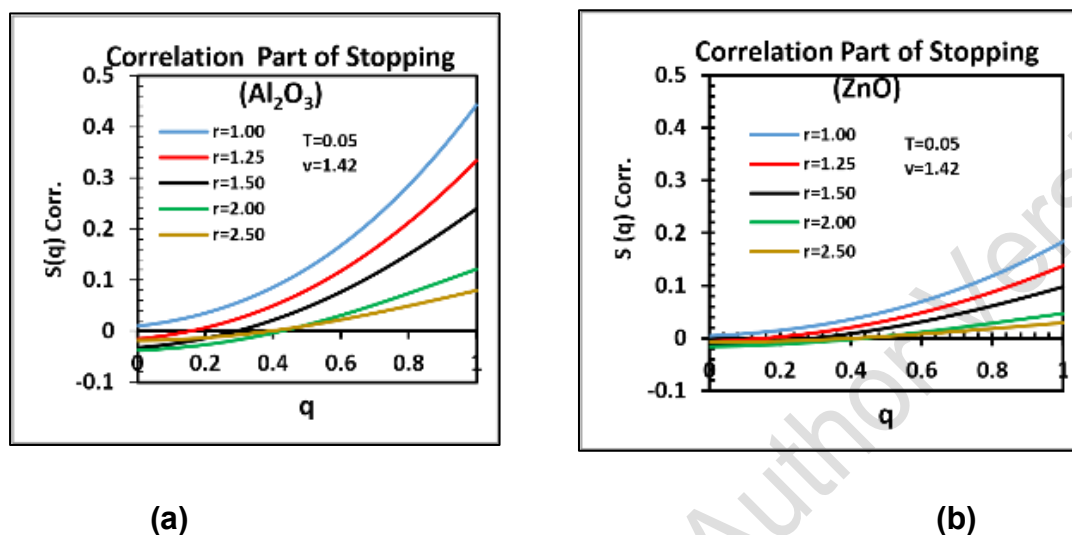
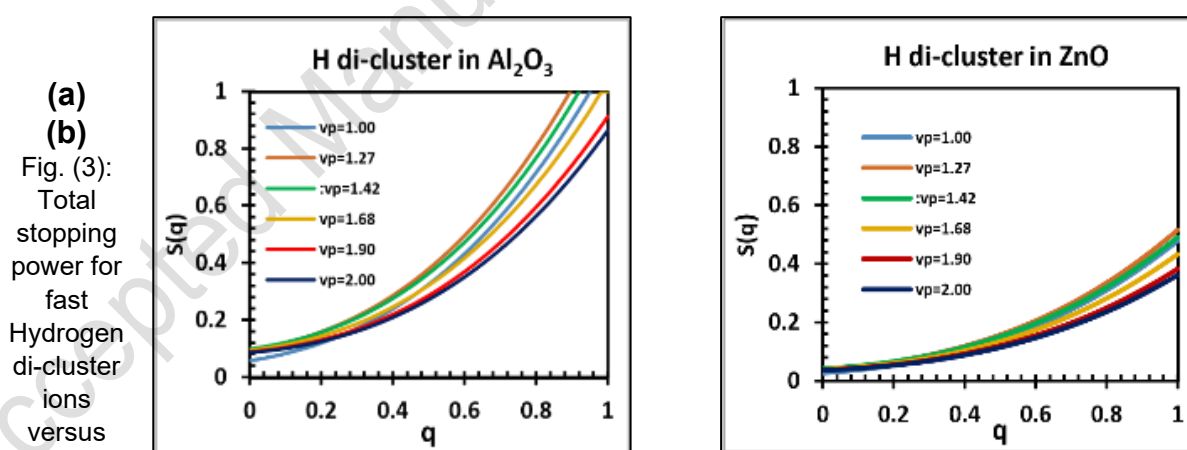


Fig. (2): Correlation of stopping power for fast Hydrogen di-cluster ions of different inter-nuclear distance r_0 in (a) Al_2O_3 , (b) ZnO

The total stopping power of compound targets for fast H- di-cluster ions is calculated with charge fraction q at different velocities as shown in Fig. 3:



(a)
(b)
Fig. (3):
Total
stopping
power for
fast
Hydrogen
di-cluster
ions
versus
ionization

fraction for velocities (1-2) in (a) Al_2O_3 , (b) ZnO

As a function of ionization fraction for different projectile velocities in Al_2O_3 and ZnO . The total effect of stopping power increases with increasing charge fraction because as the ion approaches its bare state, interaction between projectile and target electron becomes stronger too. This phenomenon is particularly noticeable in ZnO and Al_2O_3 . Besides, the stopping response depends on the projectile velocity. And this represents that both charge state

and kinematic conditions are involved in the overall energy-loss process of two compounds.

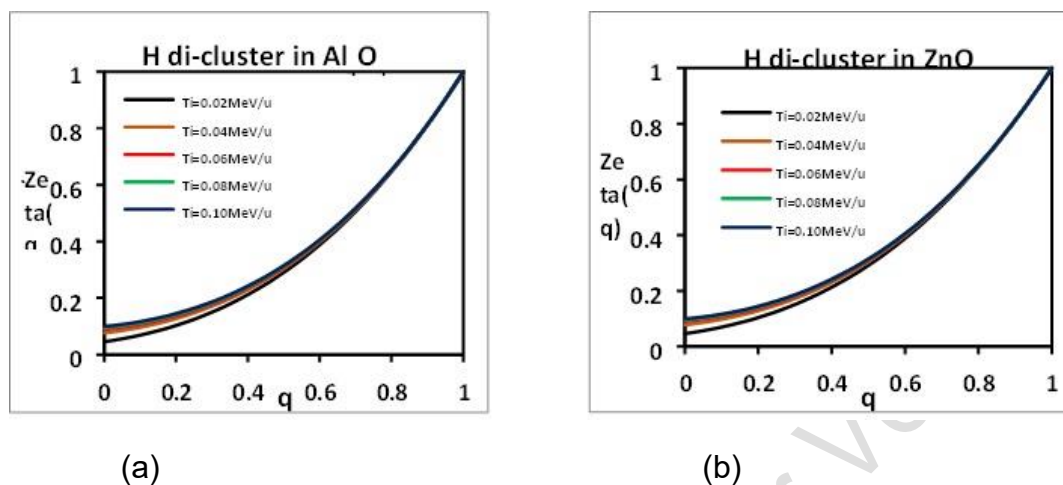


Fig. (4): Correlation stopping power for fast Hydrogen di-cluster ions in (a) Al_2O_3 , (b) ZnO

By plotting $\zeta(q)$ for various kinetic energies of the hydrogen di-cluster ion in Al_2O_3 and ZnO , figure 4 tries to show the partial stopping power as a function of effective charge. The calculation was first done for each of the elements individually and then averaged together from both constituents by using Braggs rule. The results reveal that $\zeta(q)$ depends strongly on the ionization fraction and, at lower charge states, also on the energy of the projectile beam. With increasing energy, $\zeta(q)$ tends rapidly to zero. However, higher charges at $q \rightarrow 1$, $\zeta(q)$ approaches unity at all energies considered in the region of the plot—an expected result for a projectile that is very nearly raw atomic. However, for lower values of q the dependence on energy is more pronounced, while this dependence diminishes gradually with increasing ionization.

4. Conclusion

This paper applies the dielectric formalism to investigate the stopping power and partial stopping effective charge of hydrogen practically-only fast two-lump ions in both Al_2O_3 and ZnO . From the results one can highlight that for a cluster, its stopping behavior is dominated by both self-contributions and collocations, or to put it another way the impending effect at shorter internuclear distances increases progressively closer in response. When the two protons are further apart, the magnitude of the correlation stopping power in a hydride cluster rises perhaps less than might be expected. On the other hand, the total stopping power increases as the distance between the protons is widened the partial stopping effective charge strongly depends on the charge fraction and, at lower charge states, also on the energy of the projectile. As the charge on the projectile approaches the fully ionized state, then in either compound the resultant effects tend toward unity. The more pronounced discrepancy between Al_2O_3 and ZnO is attributed to their different electronic responses. These calculations should offer valuable theoretical information about charge state-dependent energy deposition in compound oxides and be amenable for future research and applications in cluster–matter interactions.

Acknowledgements

The authors would be grateful for the support of Mustansiriyah University (www.uomustansiriyah.edu.iq) and Alnukhba University College.

Declarations Funding

This research received no specific grant from the public, commercial, or not-for-profit funding agencies.

Conflict of interest

The authors declare that they have no known competing financial interests or personal relationships that could have influenced the work reported in this paper.

REFERENCES

1. Alwan, B. J., Nsaif, N. H., Abd AL-Sada, Z. F., Al-Baraji, G. A. M., & Haddawi, S. F. (2025). Biogenic synthesis of sulfur nanoparticles using saffron flower extract and its synergistic antimicrobial activity. *Journal of Theoretical and Applied Physics*, 19(3). <https://doi.org/10.57647/j.jtap.2025.1903.32>
2. Moneta M. Stopping of slow H-to Be-like ions in an electron gas. *Nuclear Instruments and Methods in Physics Research Section B: Beam Interactions with Materials and Atoms*. 2000 Sep 1;170(1-2):28-34.
3. Rahi SK, Al-Wardy RA, Ogaili HA. The Fabrication of SeO₂ Nanoparticles from Cinnamon extract: Optical properties and its application. *Baghdad Science Journal*. 2025;22(4):1252-9.
4. Radiative transfer model application with satellite imagery for methane emission analysis. *Journal of Theoretical and Applied Physics*, 19(4) (2025). <https://doi.org/10.57647/j.jtap.2025.1904.36>
5. Rahi SK, Shaker IA, Hadi AK. The Effect of Gamma Rays on Some Electrical Properties of Polyethylene Glycol (PEG) Dissolved in Distill Water. *In Macromolecular Symposia 2022 Feb (Vol. 401, No. 1, p. 2100347)*.
6. Sigmund P, Schinner A. Binary theory of electronic stopping. *Nuclear Instruments and Methods in Physics Research Section B: Beam Interactions with Materials and Atoms*. 2002 Oct 1;195(1-2):64-90.
7. Rahi SK, Nasser ZS, Shakir IA. The effect of gamma rays in some optical and physical properties of the material (PVA) dissolved in distilled water. *Journal of global pharma technology*. 2019;11(2):593-600.
8. Moneta M, Czerbniak J. Stopping of swift ions under channeling condition: Influence of the projectile electronic structure on the effective charge. *Nuclear Instruments and Methods in Physics Research Section B: Beam Interactions with Materials and Atoms*. 2003 Aug 1;209:246-51.
9. Issanova MK, Kodanova SK, Ramazanov TS, Bastykova NK, Moldabekov ZA, Meister CV. Classical scattering and stopping power in dense plasmas: The effect of diffraction and dynamic screening. *Laser and Particle Beams*. 2016 Sep;34(3):457-66.



Accepted Manuscript (Author Version)

10. Rahi SK, Hassoni MH, Abd AN. Study effect of reinforcement and moisture on impact strength of hybrid and single polymeric composites. *Journal of Engineering and Applied Sciences*. 2018;13(18):7624-9.
11. Matias F, Fadanelli RC, Grande PL, Koval NE, Muiño RD, Borisov AG, Arista NR, Schiwietz G. Ground- and excited-state scattering potentials for the stopping of protons in an electron gas. *Journal of Physics B: Atomic, Molecular and Optical Physics*. 2017 Aug 24;50(18):185201.
12. Behar, M.; Fadanelli, R.; Nagamine, L. et al. Electronic stopping cross sections for protons in Al_2O_3 : an experimental and theoretical study. *The European Physical Journal D* 66, 247 (2012).
<https://doi.org/10.1140/epjd/e2012-30364-1>
13. Li MM, O'Connor DJ, Timmers H. A study of the charge state approach to the stopping power of MeV B, N and O ions in carbon. *Nuclear Instruments and Methods in Physics Research Section B: Beam Interactions with Materials and Atoms*. 2004 Jul 1;222(1-2):11-8.
14. Sigmund, P.; Schinner, A. Electronic stopping in oxides beyond Bragg additivity. *Nuclear Instruments and Methods in Physics Research Section B* 415, 110–116 (2018). <https://doi.org/10.1016/j.nimb.2017.11.023>
15. Sigmund P, Schinner A. Binary stopping theory for swift heavy ions. *The European Physical Journal D-Atomic, Molecular, Optical and Plasma Physics*. 2000 Nov;12(3):425-34.
16. Abril, I., Moreno-Marín, J.C., Fernández-Varea, J.M., Denton, C.D., Heredia-Avalos, S. and Garcia-Molina, R., 2007. Calculation of the energy loss of swift H and He ions in Ag using the dielectric formalism: The role of inner-shell ionization. *Nuclear Instruments and Methods in Physics Research Section B: Beam Interactions with Materials and Atoms*, 256(1), pp.172-176.
17. Matias, F.; Fadanelli, R. C.; Grande, P. L. Stopping power of cluster ions in a free-electron gas from partial-wave analysis. *Physical Review A* 98, 062716 (2018).
<https://doi.org/10.1103/PhysRevA.98.062716>
18. Shakir IA, Naser ZS. Proton single differential cross-section, electron energy loss and elastic mean free path in ZrO_2 and Al_2O_3 . In *AIP Conference Proceedings 2020 Mar 25 (Vol. 2213, No. 1, p. 020022)*. AIP Publishing LLC.

